Supplementary Information

An Enantiomeric Pair of 2D Organic-Inorganic Hybrid Perovskites with Circularly Polarized Luminescence and Photoelectric Effects

Xuan-Hui Zhao,[a‡] Xiaozong Hu,[b‡] Meng-En Sun,[b] Xi-Ming Luo,[b] Chong Zhang,[b] Gao-Song Chen,[b] Xi-Yan Dong[ab] and Shuang-Quan Zang[b*]*

[†]College of Chemistry and Chemical Engineering, Henan Polytechnic University Henan Key Laboratory of Coal Green Conversion, Henan Polytechnic University, Jiaozuo 454000, China

[‡]College of Chemistry, Zhengzhou University, Zhengzhou 450001, China

*Correspondence: dongxiyan0720@hpu.edu.cn (X. Y. Dong), zangsqzg@zzu.edu.cn (S. Q. Zang)

METHODS

Reagents and Materials Used. (1R, 2R)-(-)-1,2-Cyclohexanediamine (***R*-CHD**, 98%), (1S, 2S)-(+)-1,2-Diaminocyclohexane (***S*-CHD**, 98%) and (±)-trans-1,2-Diaminocyclohexane (***rac*-CHD**, 98%) were purchased from Bidepharm Ltd. (Shanghai, China). Lead(II) bromide ($PbBr_2$, 99%) was purchased from aladdin Ltd. (Shanghai, China). Hydrobromic acid (HBr)，ethyl acetate and Ether purchased from Kermel Ltd. (Tianjin, China).

Materials Preparation. Synthesis of $C_6H_{10}(NH_2)_2 \cdot 2HBr$. *R-/S-/rac*-cyclohexanediamine (**CHD**) (2.28 g, 20 mmol) was added in 40 mL of methanol in an ice bath, and the excess concentrated HBr aqueous solution (48%, 5.6 mL, 50 mmol) was added dropwise to the flask with vigorous stirring. After the addition of HBr, the mixture was allowed to stand in ice bath overnight. The crystals of $C_6H_{10}(NH_2)_2 \cdot 2HBr$ was obtained by rotary evaporating the residual organic solvents at 60 ℃. The crystals was collected and washed in ethyl acetate twice， Remove unreacted HBr to obtain white crystals.

Synthesis and purification of (*R*)-$C_6H_{16}N_2PbBr_4$ (***R-1***), (*S*)-$C_6H_{16}N_2PbBr_4$ (***S-1***) and $(C_6H_{16}N_2)_2Pb_2Br_8 \cdot H_2O$ (***rac-1***). Lead (II) bromide (36 mg) and $C_6H_{10}(NH_2)_2 \cdot 2HBr$ (27 mg) were mixed and dissolved in HBr (1 mL)，The mixture was placed for ultrasonic treatment to form a clear precursor solution. And the ***R/S-1*** and ***rac-1*** crystals were prepared by diffusing ether (2 mL) into the prepared precursor solution (1 mL) at room temperature for overnight. The crystals were washed with ethyl acetate and dried overnight with 60 ℃ under reduced pressure.

Device Fabrication. The single-crysal electrodes were made using SPI conductive silver paint(SPI 05002-AB) by placing the crystal between two electrodes.

Material Characterizations. Crystallographic data collection and refinement of the structure. Single-crystal X-ray diffraction measurement of ***R-1***, ***S-1*** and ***rac-1*** were performed on a Rigaku XtaLAB Pro diffractometer. Data collection and

reduction were performed using the program CrysAlisPro.[1] All the structures were solved with direct methods (SHELXS)[2] and refined by full-matrix least squares on F2 using OLEX2,[3] which utilizes the SHELXL-2015 module.[4] All the atoms were refined anisotropically. Hydrogen atoms were placed in calculated positions refined using idealized geometries and assigned fixed isotropic displacement parameters. The crystal structures are visualized by DIAMOND 3.2. Powder X-ray diffraction (PXRD) patterns of ***R-1***, ***S-1*** and ***rac-1*** were collected at room temperature in the air using an X'Pert PRO diffractometer. Fourier transform infrared (FT-IR) spectra were recorded on a Bruker TENSOR 27 FT-IR spectrometer in the 400 - 4000 cm^{-1} region. Thermogravimetry analyses (TGA) were performed on a TA Q50 system under N_2 atmosphere (flow rate = 60 mL/min) in the temperature range 30 - 800 °C at a heating rate of 10 °C/min. UV-visible diffuse reflectance spectra of samples were recorded at room temperature in the range of 240 - 800 nm using a UH4150 spectrophotometer equipped with an integrating sphere. The room temperature steady-state spectroscopy, time-resolved photoluminescence (PL), temperature-dependent emission spectra and photoluminescence quantum yield were measured on the HORIBA FluoroLog-3 fluorescence spectrometer. The circular dichroism (CD) spectra of powder samples were measured on JASCO J-1500 by potassium bromide tablet pressing method. Circularly polarized luminescence (CPL) spectra of powder samples were measured on a JASCO CPL-300. Single-crystal X-ray diffraction measurement of compounds ***R-1***, ***S-1*** and ***rac-1*** was performed on a Rigaku XtaLAB Pro diffractometer. Data collection and reduction were performed using the program CrysAlisPro.

Theoretical calculations. All the calculations was performed within the framework of the density functional theory (DFT) as implemented in the Vienna Ab initio Software Package (VASP 5.3.5) code within the Perdew–Burke–Ernzerhof (PBE) generalized gradient approximation and the projected augmented wave (PAW) method.[5-8] The cutoff energy for the plane-wave basis set was set to 450 eV. The Brillouin zone of the surface unit cell was sampled by Monkhorst-Pack (MP) grids, with k-point mesh density of $2\pi \times 0.04$ $Å^{-1}$ for structures optimizations.[9] The

convergence criterion for the electronic self-consistent iteration and force was set to 10^{-5} eV and 0.01 eV/Å, respectively.

Device Characterization. Photocurrent was measured by two-probe method with a semiconductor parameter analyzer (B1500A, Keysight), and the electrodes device is in a probe station (CGO-4, Cindbest). A 365 nm light with a power density of 1.27 mW/cm^2 was used as the light source for the current-voltage and optical switch characteristics measurements.

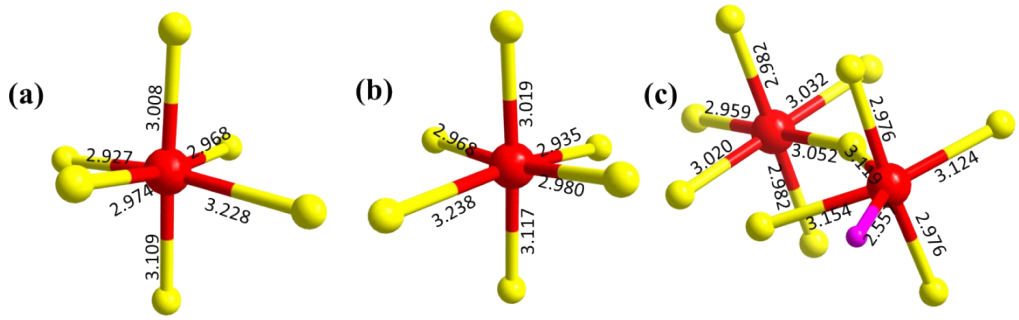

Fig. S1. Structural diagram of (a) ***R-1***, (b) ***S-1*** and (c) ***rac-1*** inorganic part and single

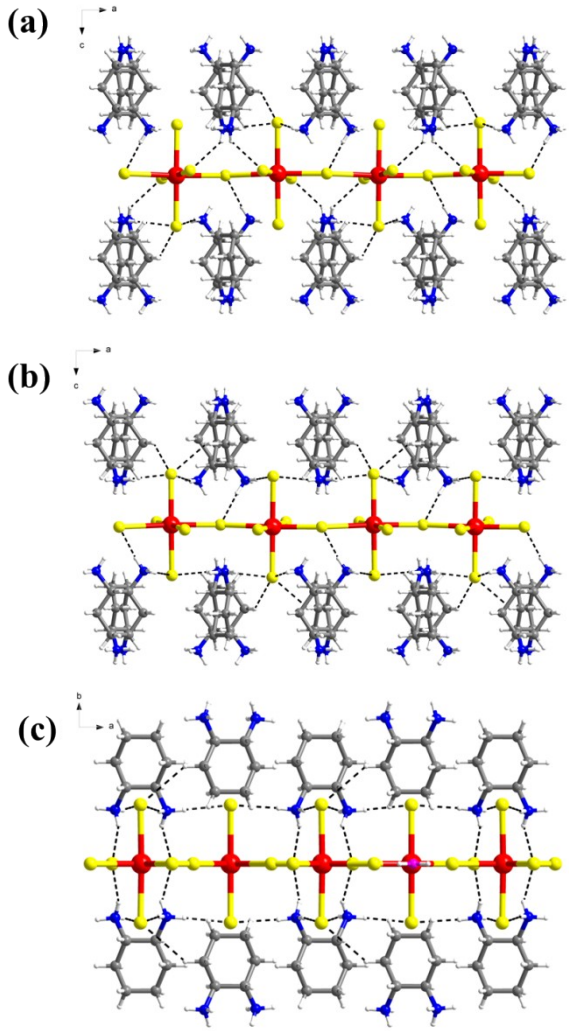

Fig. S2. Hydrogen bonding interactions of Br atoms with **CHD**$^{2+}$ spacer cations in (a) ***R-1***, (b) ***S-1*** and (c) ***rac-1***.

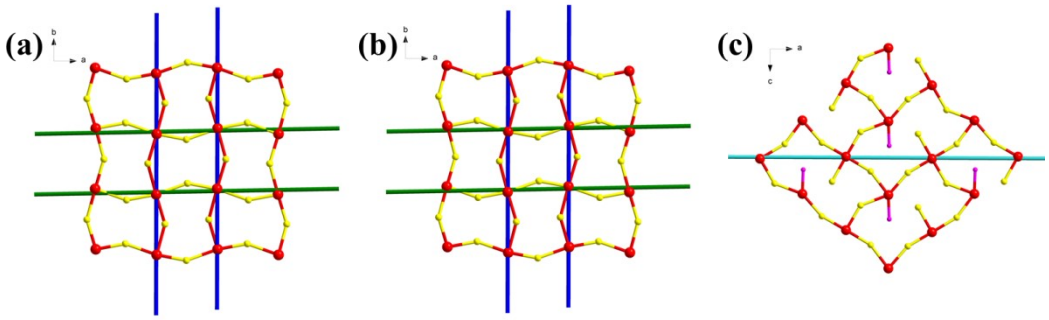

Fig. S3. Schematic diagram of the 2_1-screw axes in the inorganic layer part of (a) ***R-1***, (b) ***S-1*** and (c) ***rac-1***.

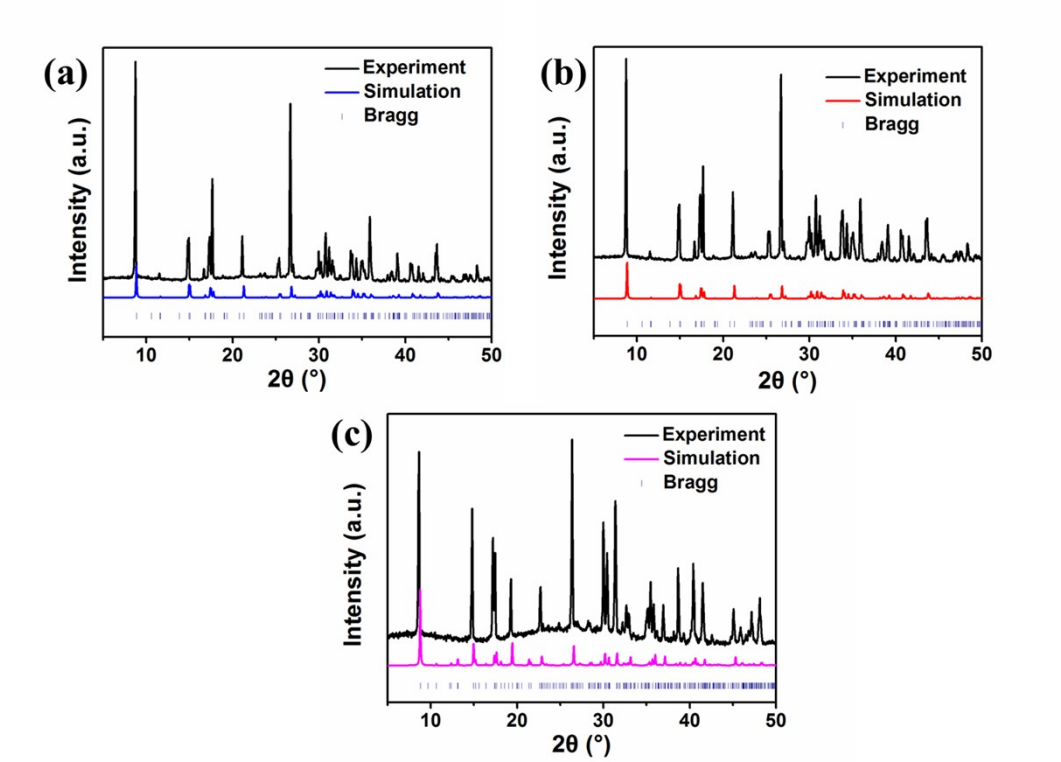

Fig. S4. PXRD patterns of our as-synthesized (a) ***R-1***, (b) ***S-1***, and (c) ***rac-1***.

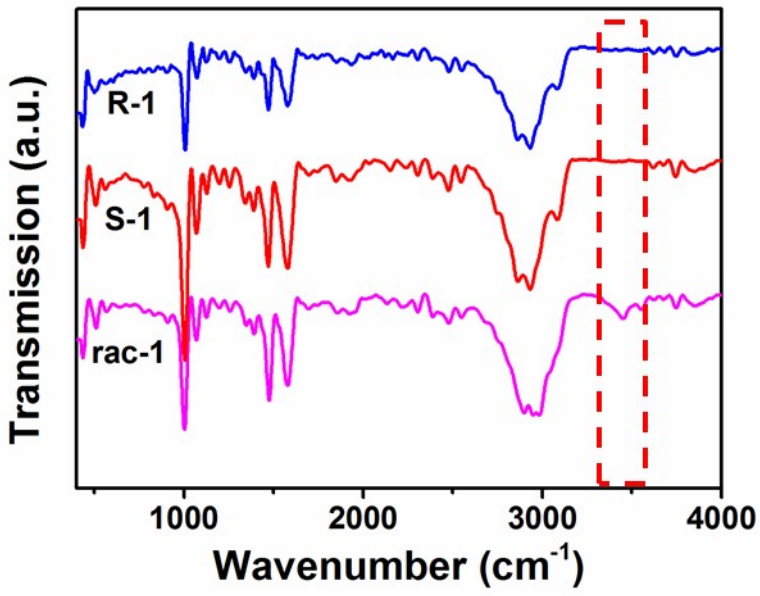

Fig. S5. The IR spectrum of ***R-1***, ***S-1*** and ***rac-1***.

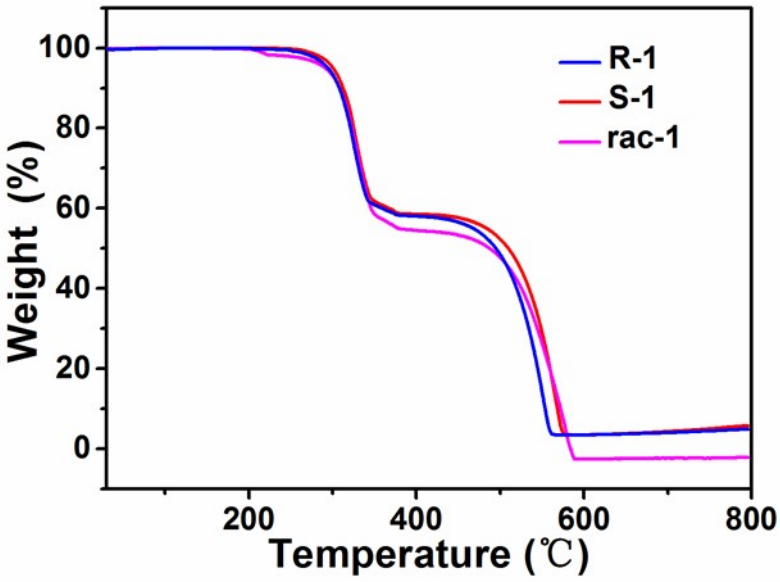

Fig. S6. The TGA curve of ***R-1***, ***S-1*** and ***rac-1***.

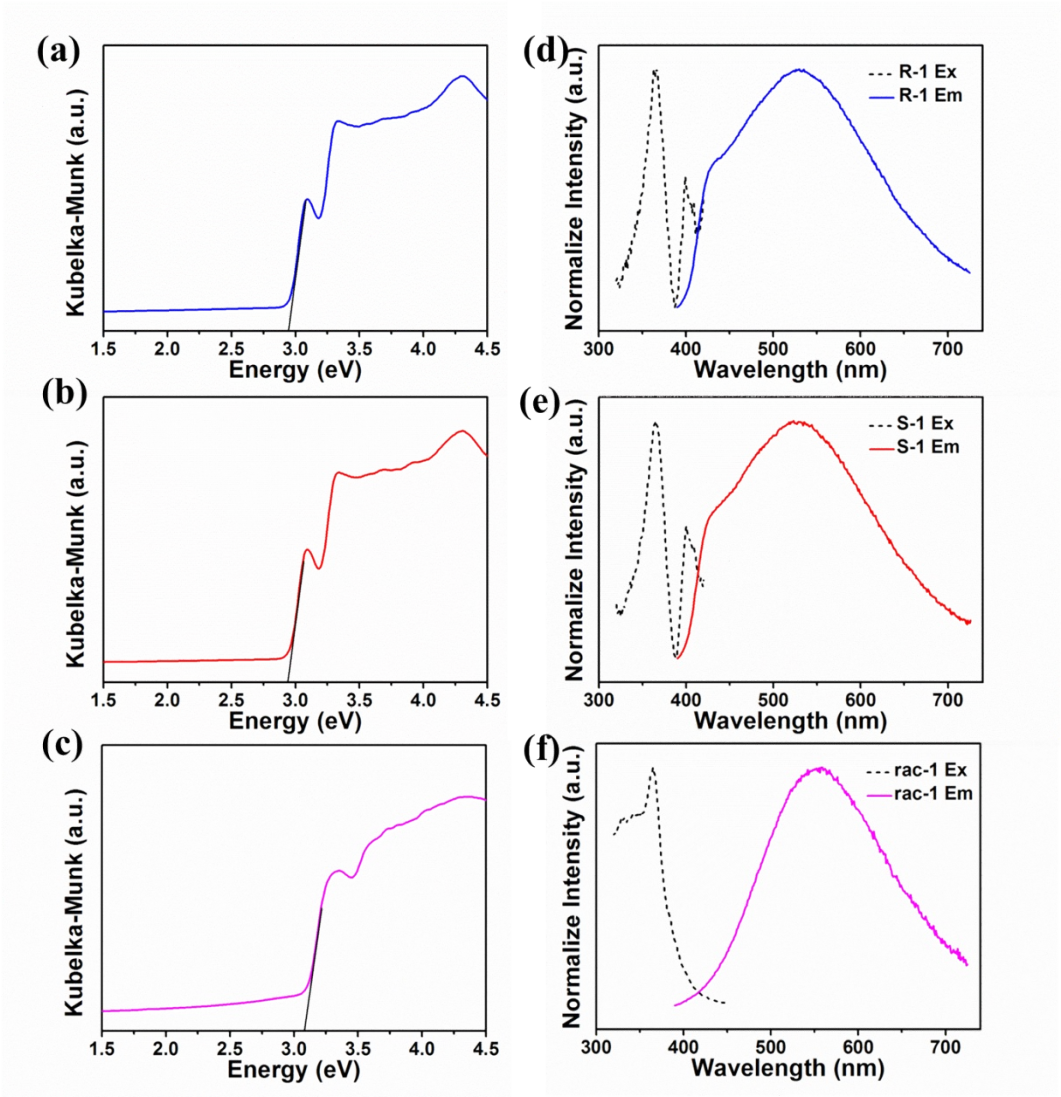

Fig. S7. Optical absorption spectra of (a) ***R-1***, (b) ***S-1*** and (c) ***rac-1***. Excitation and emission spectra of (a) ***R-1***,(b) ***S-1*** and (c) ***rac-1*** at room temperature.

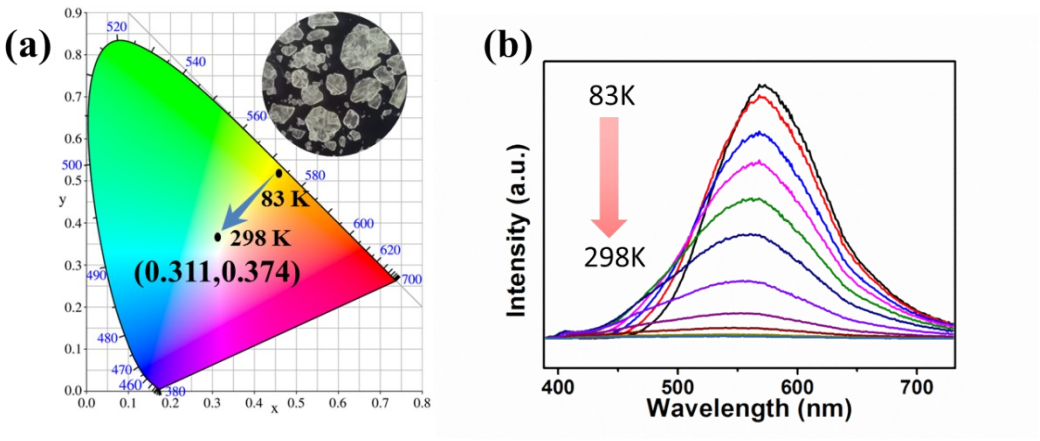

Fig. S8. (a) CIE coordinated of the emissions of ***S-1***. The illustration is a fluorescent photograph of the corresponding crystal. (b) Temperature-dependent PL spectra of ***S-1***.

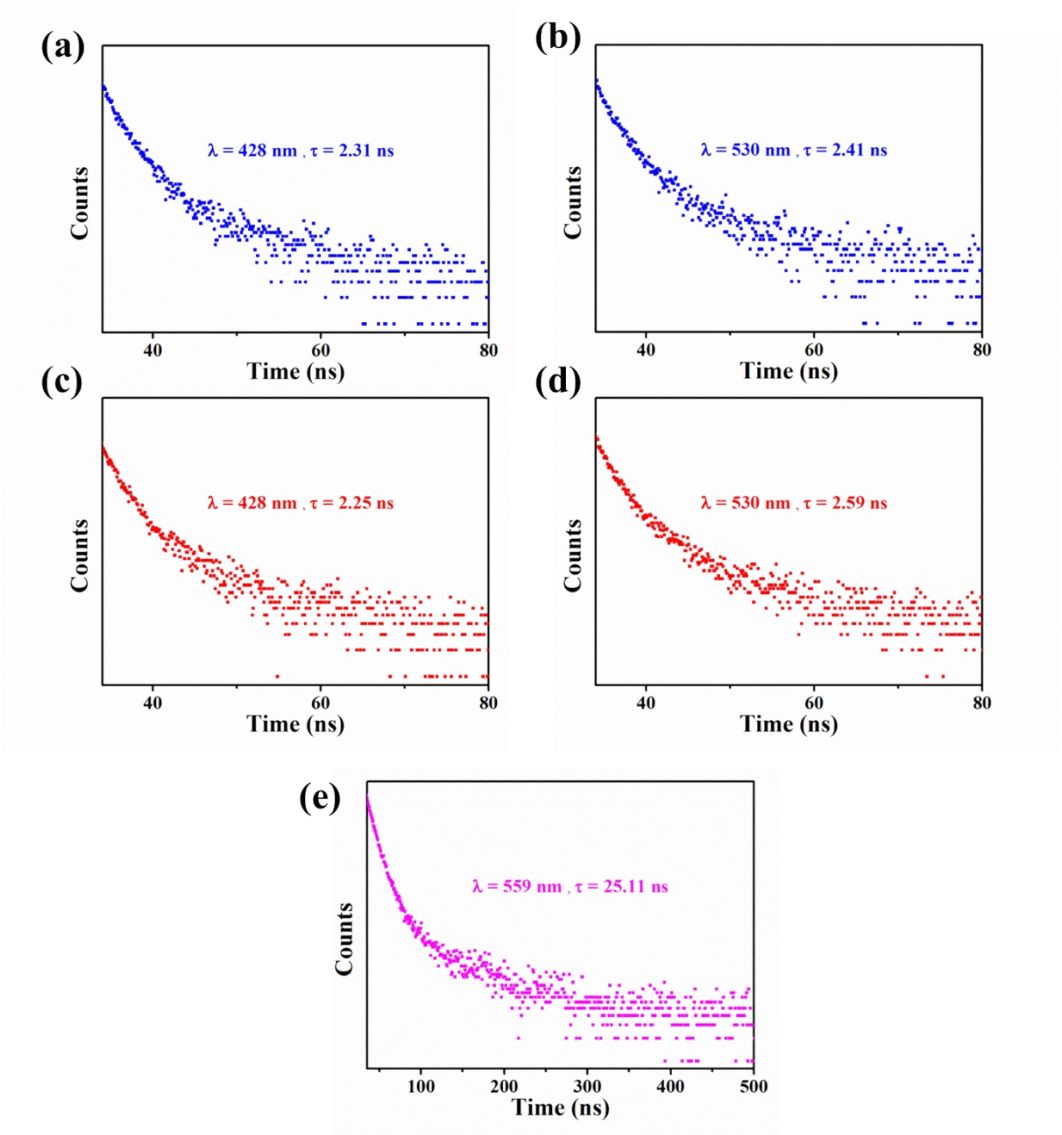

Fig. S9. Photoluminescent decay curves of (a, b) ***R-1***, (c, d) ***S-1*** and (e) ***rac-1*** at 298 K.

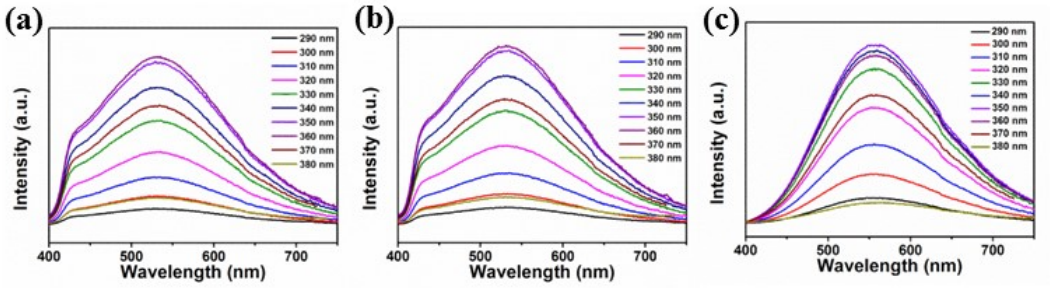

Fig. S10. Solid-state emission spectra of (a) ***R-1***, (b) ***S-1*** and (c) ***rac-1*** upon different excitation wavelengths at room temperature.

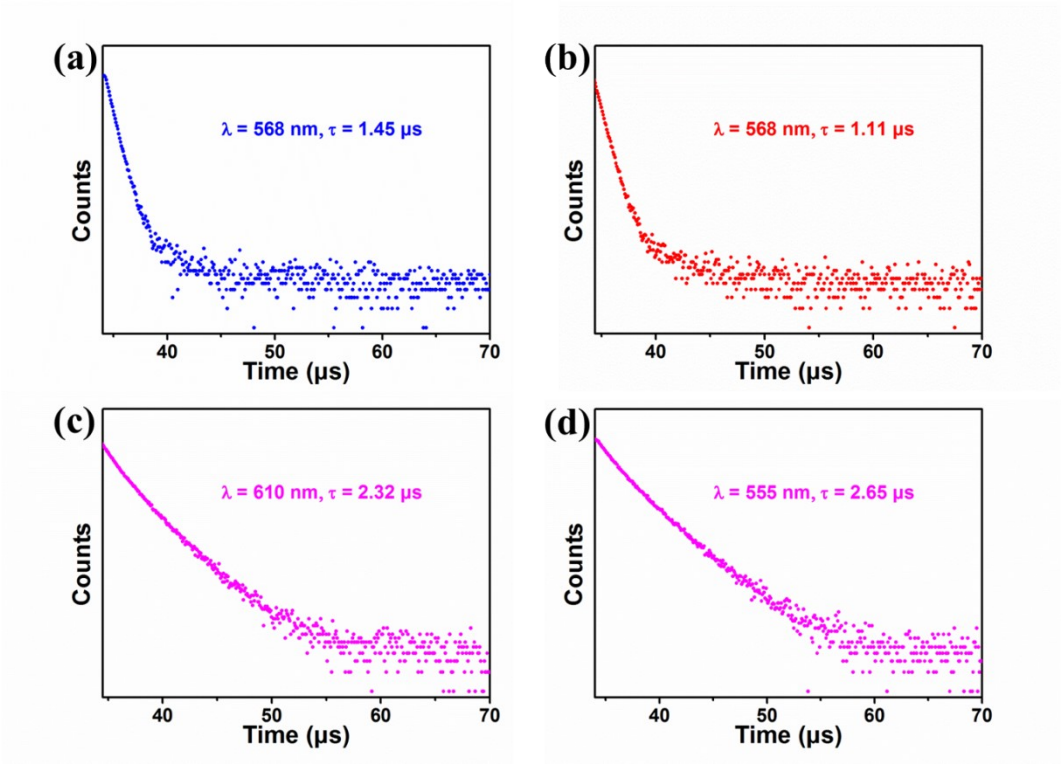

Fig. S11. Photoluminescent decay curves of (a) ***R-1***, (b) ***S-1*** and (c, d) ***rac-1*** at 83 K.

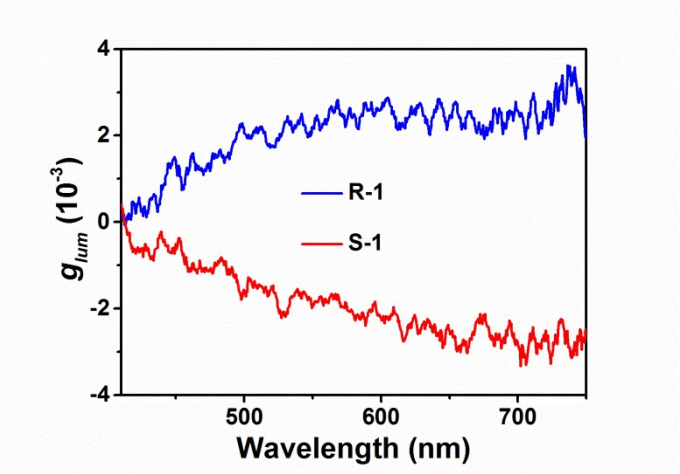

Fig. S12. The g_{lum} spectra of ***R-1*** and ***S-1***.

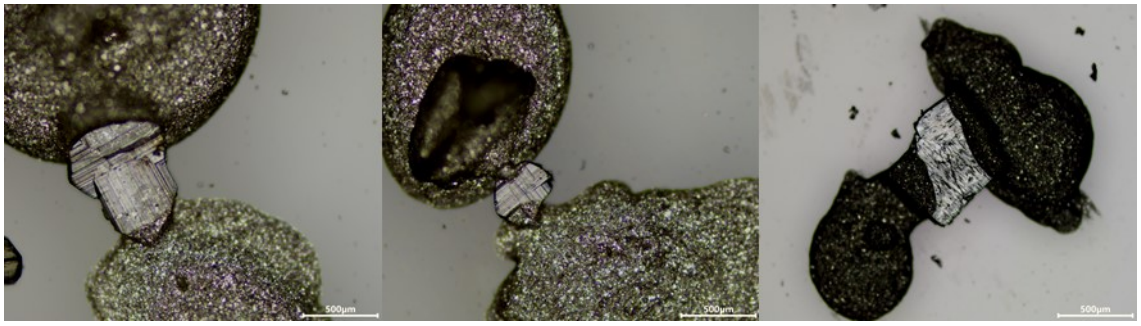

Fig. S13. From left to right are the configurations of single crystals ***R-1***, ***S-1*** and ***rac-1*** in the measurement system.

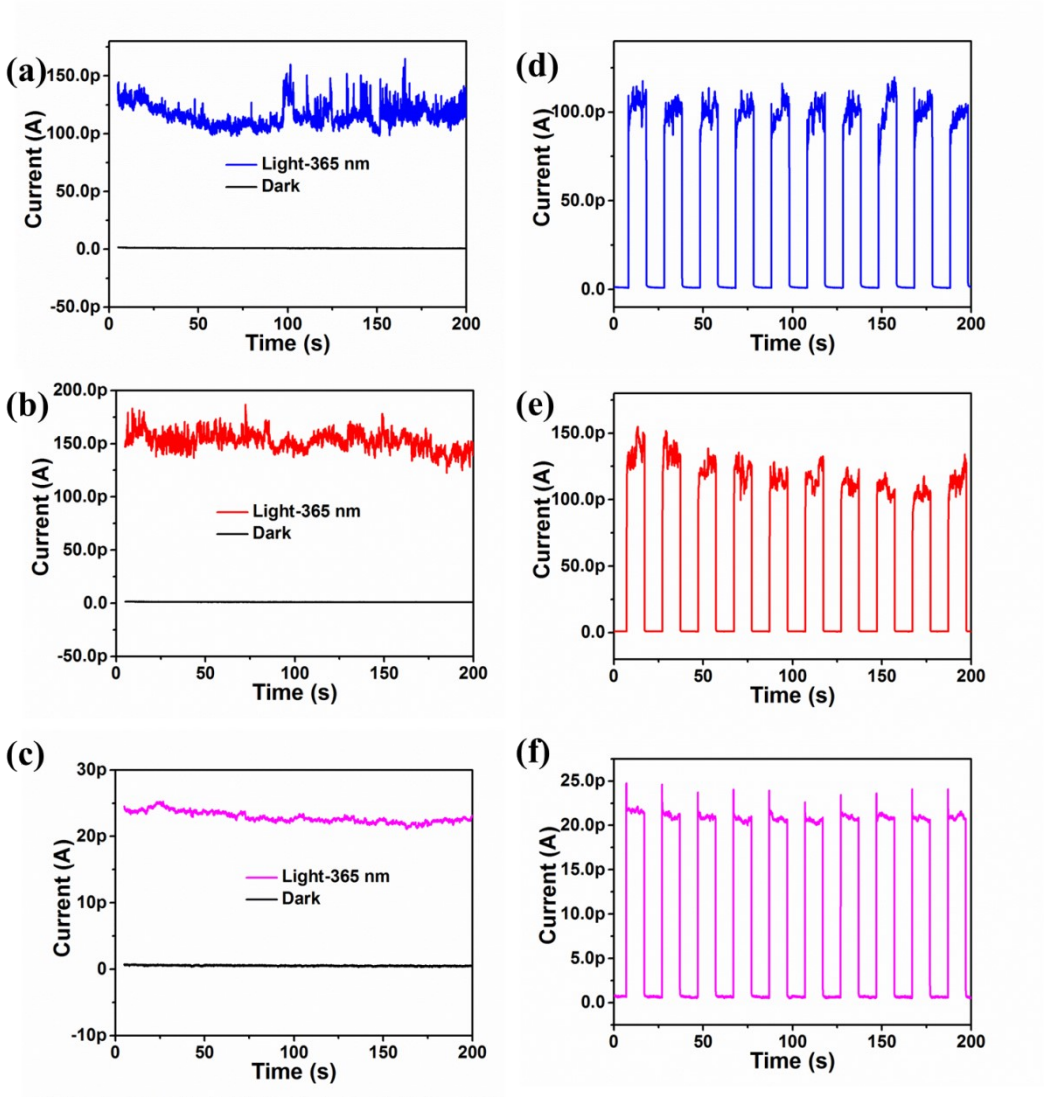

Fig. S14. The current-time curves of (a) ***R-1***, (b) ***S-1*** and (c) ***rac-1*** single-crystal device under dark and 365 nm light illumination with a power density of 1.27 mW/cm^2 at 5 V bias. Optical switch characteristic of the (d) ***R-1***, (e) ***S-1*** and (f) ***rac-1*** under a 365 nm light irradiation with a power density of 1.25 mW/cm^2 at 5 V bias.

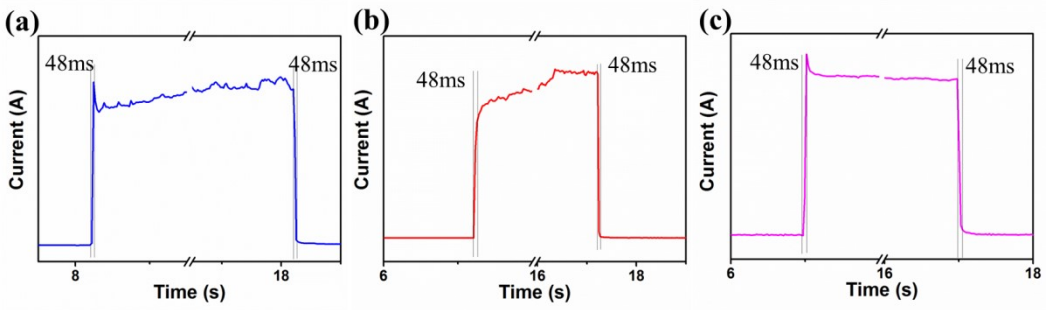

Fig. S15. Single-cycle photoresponse of (a) ***R-1***, (b) ***S-1*** and (c) ***rac-1***.

Table S1. Experimental hydrogen bonding parameters single crystal X-ray structures for various 2D HOIPs studied in this work. The subscripts 'eq' and 'ax' indicate equatorial and axial directions respectively.

Compound	H-bond	length (Å)	angle at H (°)
R-1	N-H---Br_{eq}	2.653	140.22
	N-H---Br_{eq}	2.575	152.12
	N-H---Br_{ax}	2.448	171.24
	N-H---Br_{ax}	2.434	160.68
	N-H---Br_{ax}	2.434	160.75
	N-H---Br_{ax}	2.468	168.31
	C-H---Br_{ax}	3.005	139.67
	C-H---Br_{ax}	3.121	142.53
	C-H---Br_{ax}	3.023	139.72
	C-H---Br_{ax}	3.127	139.59
S-1	N-H---Br_{eq}	2.671	140.82
	N-H---Br_{eq}	2.571	153.89
	N-H---Br_{ax}	2.443	159.70
	N-H---Br_{ax}	2.450	172.16
	N-H---Br_{ax}	2.452	158.28
	N-H---Br_{ax}	2.471	166.92
	C-H---Br_{ax}	3.019	140.11
	C-H---Br_{ax}	3.026	140.66
rac-1	N-H---Br_{eq}	2.527	158.34
	N-H---Br_{eq}	2.602	151.73
	N-H---Br_{ax}	2.490	172.72
	N-H---Br_{ax}	2.477	162.05
	N-H---Br_{ax}	2.490	171.04
	N-H---Br_{ax}	2.495	157.94
	C-H---Br_{ax}	3.057	140.74
	C-H---Br_{ax}	3.069	138.16
	O-H---Br_{eq}	2.518	158.51
	O-H---Br_{eq}	2.662	150.71

Table S2. Table of partial bond length range and distortion parameters in ***R/S-1*** and ***rac-1***.

Compound	Pb-Br length range/Å	Pb-O length range/Å	Br-Pb-Br angle range/°	O-Pb-Br angle range/°	λ_{oct}	σ^2
R-1	2.927-3.228	-	82.40-99.75	-	1.15×10^{-3}	23.65
S-1	2.935-3.238	-	81.93-100.33	-	1.17×10^{-3}	25.71
rac-1	2.959-3.052	2.557	73.481-91.582	71.574-136.716	1.17×10^{-4}	0.81
					4.67×10^{-3}	275.58

Table S3. Emission wavelength (λ_{em}), lifetimes (τ) and the corresponding fractional contributions (%) of the solid state samples at 298 K, respectively (χ^2: fitting parameter). And the PLQY of ***R-1***, ***S-1*** and ***rac-1*** at room temperature.

Compound 298K	λ_{em} (nm)	χ^2	τ_1 (%)	τ_2 (%)	τ	PLQY (%)
R-1	428	1.00	1.22 *ns* (76.42)	5.86 *ns* (23.58)	2.31 *ns*	1.33
	530	1.14	1.26 *ns* (77.01)	6.28 *ns* (22.99)	2.41 *ns*	
S-1	428	1.04	5.98 *ns* (21.13)	1.13 *ns* (76.87)	2.25 *ns*	1.44
	530	1.02	1.25 *ns* (76.32)	6.91 *ns* (23.68)	2.59 *ns*	
rac-1	559	1.02	10.60 *ns* (82.51)	93.57 *ns* (17.49)	25.11 *ns*	8.45

Table S4. Emission wavelength (λ_{em}), lifetimes (τ) and the corresponding fractional contributions (%) of the solid state samples at 83 K, respectively (χ^2: fitting parameter).

Compound-83K	λ_{em} (nm)	χ^2	τ_1 (%)	τ_2 (%)	τ
R-1	568	1.16	0.65 *μs* (91.46)	10.00 *μs* (8.54)	1.45 *μs*
S-1	568	1.10	0.66 *μs* (92.03)	6.39 *μs* (7.97)	1.11 *μs*
rac-1	555	1.16	1.51 *μs* (29.89)	3.13 *μs* (70.11)	2.65 *μs*
	610	1.17	1.54 *μs* (47.85)	3.03 *μs* (52.15)	2.32 *μs*

Supplementary References

1 CrysAlisPro, Version 1.171.36.31. Agilent Technologies Inc., Santa Clara, CA, USA 2012.

2 G. M. Sheldrick, *Acta Cryst. A,* 2008, **64**, 112−122.

3 O. V. Dolomanov, L. J. Bourhis, R. J. Gildea, J. A. K. Howard and H. Puschmann, *J. Appl. Cryst.,* 2009, **42**, 339−341.

4 G. M. Sheldrick, *Acta Cryst.* C, 2015, **71**, 3−8.

5 J. P. Perdew, K. Burke and M. Ernzerhof, *Phys. Rev. Lett.,* 1996, **77**, 3865−3868.

6 B. Hammer, L. B. Hansen and J. K. Nørskov, *Phys. Rev. B,* 1999, **59**, 7413−7421.

7 P. E. Blöchl, Phys. Rev. B, 1994, **50**, 17953−17979.

8 G. Kresse and D. Joubert, *Phys. Rev. B,* 1999, **59**, 1758−1775.

9 H. J. Monkhorst and J. D. Pack, *Phys. Rev. B,* 1976, **13**, 5188−5192.